Target Tracking Using Particle Filtering and CAZAC Sequences

Ioannis Kyriakides*, Ioannis Konstantinidis†, Darryl Morrell‡, John J. Benedetto†, and Antonia Papandreou-Suppappola*
*Department of Electrical Engineering, Arizona State University, Tempe, AZ 85287, USA, i.kyriakides@asu.edu
†Norbert Wiener Center, Department of Mathematics, University of Maryland, College Park, MD 20742, USA
‡Department of Engineering, Arizona State University, Engineering, Mesa, AZ 85212, USA

***Abstract*— When tracking targets in radar, the selection of the transmitted waveform and the method of processing the return signal are two of the design aspects that affect measurement accuracy. Increased measurement accuracy results in enhanced tracking performance. In this paper, we apply sequential Monte Carlo methods to propose matched filtering operations in the delay-Doppler space where a target is expected to exist. Moreover, in the case of thresholding the measurements, these methods are used to form resolution cells that have the shape of the probability of detection contour. These methods offer an advantage over traditional radar tracking methods that form tessellating resolution cells to approximate the probability of detection contours, and exhaustively perform matched filtering operations over the entire delay-Doppler space. With the use of a Björck constant amplitude zero-autocorrelation (CAZAC) sequence, a high resolution measurement is attained and the use of thresholding is avoided. This is an advantage over commonly used waveforms such as linear frequency modulated chirps (LFMs). We examine the properties of Björck CAZACs and demonstrate improved tracking performance over LFMs in a single target tracking scenario.**

I. Introduction

A typical target tracking radar system transmits a waveform and processes its return in order to extract information on the range and range rate of the target with respect to the radar sensors. The measurement accuracy in the range and range rate depends on the waveform used and the processing method of the return signal.

The more localized ambiguity function [1] a waveform has in the delay-Doppler space, the more accurate information it provides on the range and range rate of a given target with respect to the radar system. Therefore, carefully selecting the transmitted waveform is imperative to the design of an accurate radar system. In this paper, we enhance measurement accuracy with the use of Björck CAZAC sequences [2] that have a highly concentrated ambiguity function in the delay-Doppler space. This results in smaller resolution cells and thus smaller measurement errors as compared to the case of waveforms typically used in radar, such as linear frequency modulated (LFM) waveforms.

The traditional method for processing radar signal returns is to separate the delay-Doppler space into tessellating shaped resolution cells centered on a fixed grid of delay and Doppler locations. A detection or no detection is then obtained for each resolution cell based on the thresholded output of a matched filter placed on the centroid of the cell. The resolution cells are usually parallelograms that are shaped and oriented in such a way as to efficiently enclose a probability of detection contour. This contour is formed by thresholding the ambiguity function of the waveform [3], [4]. When a tessellating shape does not exactly match the shape of the probability of detection contour, such as in the case of LFMs, this results in measurement errors. Moreover, matched filter outputs at all grid points need to be exhaustively evaluated, and thresholding the matched filter output introduces further measurement errors.

Physical systems such as the one studied in this paper are more accurately represented by non-linear, non-Gaussian models, which can be solved more effectively with sequential Monte Carlo methods such as particle filtering methods [5]. In our approach, each proposed particle location from the particle filter in the target state space is associated with a matched filter location in the delay-Doppler space. Using the proposed matched filter locations and the exact shape of the probability of detection contour, we form resolution cells. These cells propagate to areas of interest based on prior information on the target state and the measurements, rather than being fixed on a grid. This is done using a sampling importance resampling particle filter (SIRPF) with an LFM waveform. The same benefits emerge when using a likelihood particle filter (LPF) with Björck CAZAC sequences. Therefore, measurement errors due to the approximation of the probability of detection contours as parallelograms are eliminated, and an exhaustive search over all grid points is omitted. In the case of a Björck CAZAC, the need of thresholding is also avoided. We demonstrate through simulations that the use of the Björck CAZAC for single target tracking using particle filtering and radar measurements offers significant tracking performance gains as compared to the use of an LFM waveform.

The paper is organized as follows. In Section II, we describe the state space formulation of the single target tracking approach using radar. In Section III, we describe the LFM waveform and CAZAC sequences. We describe the SIRPF and the LPF in Section IV, and evaluate their performance using simulations in Section V.

II. Problem Formulation

A. Motion Model

We consider a single target moving in a two-dimensional plane. The dynamics of the target are modeled using a nearly constant velocity motion model in Cartesian coordinates. Specifically, the state vector for the target at time step k, $k = 1, ..., K$, is given by: $\mathbf{x}_k = [x_k \ \dot{x}_k \ y_k \ \dot{y}_k]^T$, where x_k, y_k are the positions in the x and y coordinates, and $\dot{x}_k$, $\dot{y}_k$ are the corresponding velocities. The motion is formulated as:

$$\mathbf{x}_k = \mathbf{F}\mathbf{x}_{k-1} + \mathbf{Q}\mathbf{v}_{k-1}, \tag{1}$$

where

$$\mathbf{F} = \begin{bmatrix} 1 & \delta t & 0 & 0 \\ 0 & 1 & 0 & 0 \\ 0 & 0 & 1 & \delta t \\ 0 & 0 & 0 & 1 \end{bmatrix}$$

[0]This work was supported under MURI Grant No. AFOSR FA9550-05-1-0443.

and δt is the time difference between state transitions. The matrix $\mathbf{Q}$ is the process noise covariance matrix, and $\mathbf{v}_k$ denotes a zero-mean, unit variance Gaussian process that models errors in velocity, possibly due to unknown acceleration; in this work, we restrict $\mathbf{Q}$ to be diagonal. The model in (1) can be used to determine the kinematic prior distribution $p(\mathbf{x}_k|\mathbf{x}_{k-1})$.

B. Measurement Model

A radar system collects information regarding the range and range rate of a target relative to the radar sensors by transmitting signal pulses and processing the return reflected by a target of interest. The return signal bears information on the range of a target $r_{l,k}$ relative to a sensor $l = 1, \ldots, L$ of the radar system in the form of a time delay $\tau_{l,k}$ relative to the transmitted signal as $r_{l,k} = \frac{c\tau_{l,k}}{2}$, where c is the velocity of propagation of the signals. Moreover, it bears information and on the range rate of a target $\dot{r}_{l,k}$ in the form of a Doppler shift $\nu_{l,k}$ as $\dot{r}_{l,k} = -\frac{c\nu_{l,k}}{2f_c}$, where f_c is the carrier frequency. In this section, we explain how the return signal is processed by a radar system and how information on range and range rate is obtained.

We assume that at every time step k a radar waveform $s(m), m = 1, \ldots, M$, where M is the total number of samples of the waveform, is transmitted from L sensors. The return signals that are reflected from the target with a delay $\tau_{l,k}$ and Doppler $\nu_{l,k}$ arriving at the sensors are:

$$d_{l,k}(m) = A(m)s(m - \tau_{l,k})e^{j2\pi(m-\tau_{l,k})\nu_{l,k}/M} + v(m)$$

for $m = 1, \ldots, M$, where $A(m)$ is a sum of random complex returns from many different target scatterers, according to the Swerling I model [6]. Therefore, $A(m)$ is assumed to be zero-mean, complex Gaussian with known variance $2\sigma_A^2$ and $v(m)$ is zero-mean complex Gaussian noise with variance $2N_0$. The return signal when no target is present is given by

$$d_{l,k}(m) = v(m), \ m = 1, \ldots, M.$$

The return signal is passed through matched filters located at different time (τ_0) and Doppler (ν_0) shift locations as:

$$\mathbf{y}_{\tau_0,\nu_0,l,k} = |\frac{1}{M}\sum_{m=0}^{M'} d(m)s^*(m - \tau_0)e^{-j2\pi(m-\tau_0)\nu_0/M}|^2$$

with $M' > M$ that should be large enough to accommodate a maximum delay of a signal reflected from a target. Specifically, the factor $\frac{1}{M}\sum_{m=0}^{M'} d(m)s^*(m-\tau_0)e^{-j2\pi(m-\tau_0)\nu_0/M}$ in the absence of a target is zero mean, complex Gaussian with variance $2N_0\xi$, where ξ is the energy of the transmitted signal. In the presence of a target, it is zero mean, complex Gaussian with variance $\sigma_1^2 = \sigma_0^2(1+\frac{2\sigma_A^2\xi^2}{\sigma_0}\mathcal{A}(\tau_0-\tau_{l,k}, \nu_{l,k}-\nu_0))$ where $\mathcal{A}(-\tau, \nu)$ is the time-reversed ambiguity function [3] given as:

$$\mathcal{A}(-\tau, \nu) = |\frac{1}{M}\sum_{m=0}^{M} s^*(m)s(m - \tau)e^{j2\pi(m-\tau)\nu/M}|^2.$$

The matched filter statistic $\mathbf{y}_{\tau_0,\nu_0,l,k}$ is exponentially distributed. Therefore,

$$p(\mathbf{y}_{\tau_0,\nu_0,l,k}|\mathbf{x}_k) = \begin{cases} \frac{1}{2\sigma_1^2}e^{-\frac{\mathbf{y}_{\tau_0,\nu_0,l,k}}{2\sigma_1^2}} & \text{, if target present} \\ \frac{1}{2\sigma_0^2}e^{-\frac{\mathbf{y}_{\tau_0,\nu_0,l,k}}{2\sigma_0^2}} & \text{, if target not present.} \end{cases}$$

If we threshold the matched filter output, we have:

$$\bar{\mathbf{y}}_{\tau_0,\nu_0,l,k} = \begin{cases} 1, & \text{if } \mathbf{y}_{\tau_0,\nu_0,l,k} \geq \mathcal{T} \\ 0, & \text{if } \mathbf{y}_{\tau_0,\nu_0,l,k} < \mathcal{T} \end{cases}$$

obtaining a detection (1) or no detection (0). We can calculate a threshold $\mathcal{T} = -2\sigma_0^2\ln(P_f)$, where ln is the natural logarithm, based on a probability of false alarm (P_f). The probability of detection is given by $P_d = P_f^{1/(1+\text{SNR } A(\tau_0-\tau_{l,k},\nu_{l,k}-\nu_0))}$. The signal-to-noise ratio (SNR) is defined as $\text{SNR} = \frac{\sigma_A^2\xi}{N_0}$, where ξ is the energy of the transmitted signal [3].

Traditionally, the delay-Doppler space is exhaustively overlaid with tessellating cells from which we obtain detections in order to infer the location of a target in the range-range rate space. The estimate of a target's position is based on averaging the grid locations, where a detection is obtained. The authors of [3], [4] use the thresholded ambiguity function shape and orientation to create these tessellating shaped cells. This is because, excluding the effect of noise and the scatterers, the matched filter statistic is proportional to the ambiguity function. However, a tessellating shaped cell does not exactly match the shape of the thresholded ambiguity function. Therefore, increased measurement errors follow from this method. In the proposed methods, we explain how this is avoided using particle filtering and unthresholded measurements with Björck CAZAC sequences.

III. Waveform Design

We are interested in waveforms having concentrated ambiguity functions to provide good resolution in both range and range rate. In this section, we describe a popular type of waveform in radar, the linear LFM chirp. Furthermore, we describe CAZAC sequences and their many useful properties that make them a favorable choice in radar sensing.

A. LFM Sequences

In an LFM sequence, the frequency linearly increases or decreases with the duration of the waveform. The LFM is described by the equation

$$s(m) = \exp\left(j2\pi\frac{(f_b - f_a)((m-1)^2 - (\frac{M}{2}-1)^2)}{2(M-1)}\right)$$

for $m = 1, \ldots, M$, where f_a and f_b are respectively the initial and final normalized frequencies of the waveform. The normalized frequency is equal to the actual frequency in Hz divided by the sampling frequency. Thus, the minimum and maximum normalized frequencies are 0 and 0.5, respectively.

B. Björck CAZAC Sequences

Björck sequences are quadratic residue sequences of prime length $M = p$. For prime $p = 1 \mod 4$ the Björck sequence is given by: $u(m) = e^{j2\pi\theta\left(\frac{m}{p}\right)}$, $m = 1, \ldots, M$, where $\theta = \arccos(\frac{1}{1+\sqrt{p}})$, and $\left(\frac{m}{p}\right)$ is the Legendre symbol:

$$\left(\frac{m}{p}\right) = \begin{cases} 1, & \text{if } m = 0 \ (mod\ p) \\ 1, & \text{if } m \text{ is a square } (mod\ p) \\ -1, & \text{if } m \text{ is not a square } (mod\ p) \end{cases}$$

Björck sequences are called *constant amplitude zero-autocorrelation* (CAZAC) since $|u(m)| = 1$ for all $m = 1, \ldots, M$, and $\frac{1}{M}\sum_{m\mathbb{Z}_M} u(\mu + m)u^*(m) = 0$, for all $\mu \neq 0$, where addition is modulo M. They are examples of small alphabet CAZACs, because they assume at most three distinct values. For primes $p = -1 \mod 4$, we can construct CAZAC sequences with an alphabet of two letters:

$$u[m] = \begin{cases} 1 & \text{if } m \text{ is a square } (mod\ p) \\ e^{j2\pi\theta}, & \text{if } m \text{ is not a square } (mod\ p) \text{ [2].} \end{cases}$$

Small alphabet CAZACs decouple the effect of delay and Doppler (see Figure 1) better than quadratic phase sequences like the Frank-Zadoff-Chu [7] and LFM sequences. Therefore, Björck CAZAC codes are an attractive choice for target tracking with radar. They have a constant amplitude, which allows the transmission of peak power throughout the duration of the code. This allows more power to be transmitted in the scene, increasing the SNR [8]. Moreover, they exhibit very tight localization in the delay-Doppler space that enhances the range-range rate resolution of the measurements. Specifically, the ambiguity function of the Björck CAZAC exhibits a large spike in the (0,0) bin of the discrete delay-Doppler space with very small sidelobes.

IV. Tracking Algorithm

We describe a sampling importance resampling particle filter (SIRPF) and a likelihood particle filter (LPF) [5] for the radar tracking problem. The SIRPF usually makes use of the prior density as the importance density. However, when the likelihood is much more concentrated than the prior, the probability of a particle proposed by the prior to fall in a location where the likelihood has a significant value is very small. Therefore, the LPF is employed to use the likelihood as the importance density. In the case of the LFM waveform, the likelihood is broad due to the spread of the ambiguity function. Therefore, the SIRPF method can be used. In the case of the Björck CAZAC, however, the likelihood is very peaked as compared with the prior and the LPF is employed. The LPF in this setting is more computationally expensive than the SIRPF. However, the use of the LPF with the Björck CAZAC results in significant gains in tracking performance as compared to using the SIRPF with an LFM waveform.

A. SIR Particle Filter

Every particle is a hypothesis on the state $\mathbf{x}_k$ of a target denoted by $\mathbf{x}_k^n$ where $n = 1, \ldots, N$ is the particle index and N is the total number of particles used. Having a proposed state $\mathbf{x}_{k-1}^n$ at time $k-1$ for each particle, we independently propagate each particle $n = 1, \ldots, N$ to time step k using: $\mathbf{x}_k^n = \mathbf{F}\mathbf{x}_{k-1}^n + \mathbf{Q}\mathbf{v}_k$ which amounts to sampling from a Gaussian distribution $q(\mathbf{x}_k|\mathbf{x}_{k-1}^n)$ with mean $\mathbf{F}\mathbf{x}_{k-1}^n$ and covariance matrix $\mathbf{Q}$, called the importance density [5]. The generated states $\mathbf{x}_k^n$ correspond to range and range rate

$$r_{l,k}^n = \sqrt{(\chi_l - x_k^n)^2 + (\psi_l - y_k^n)^2}$$

$$\dot{r}_{l,k}^n = (\dot{x}_k^n(x_k^n - \chi_l) + \dot{y}_k^n(y_k^n - \psi_l))/r_{l,k}^n$$

which in turn correspond to delay and Doppler shift indices $\tau_{l,k}^n = \text{round}(\frac{2\dot{r}_{l,k}^n/c}{\Delta\tau})$ and $\nu_{l,k}^n = \text{round}(\frac{-2f_c\dot{r}_{l,k}^n/c}{\Delta\nu})$, respectively. Here, χ_l and ψ_l are the x and y locations of the l sensor. The output of the matched filter at a proposed delay-Doppler location by a particle n and with respect to a sensor l is:

$$\mathbf{y}_{l,k}^n = |\frac{1}{M}\sum_{m=0}^{M} d(m)s^*(m - \tau_{l,k}^n)e^{-j2\pi(m-\tau_{l,k}^n)\nu_{l,k}^n/M}|^2.$$

The likelihood function for each particle $n' = 1, \ldots, N$ is given by $p^{n'}(\{\{\mathbf{y}_{l,k}^n\}_{n=1}^N\}_{l=1}^L|\mathbf{x}_k^1, \ldots, \mathbf{x}_k^{n'}, \ldots, \mathbf{x}_k^N)$. Here, the hypothesis of particle n' is that the state equals $\mathbf{x}_k^{n'}$, while $\{\{\mathbf{y}_{l,k}^n\}_{n=1}^N\}_{l=1}^L$ are the measurements obtained from matched filters at the delay-Doppler location defined by the particle proposed target state vectors $\{\mathbf{x}_k^n\}_{n=1}^N$. This likelihood

TABLE I
SIR Particle Filter [5]

- For each particle $n = 1, \ldots, N$
  - Sample $\mathbf{x}_k^n \sim q(\mathbf{x}_k|\mathbf{x}_{k-1}^n)$
  - For each sensor $l = 1, \ldots, L$
    - $r_{l,k}^n = \sqrt{(\chi_l - x_k^n)^2 - (\psi_l - y_k^n)^2}$
    - $\dot{r}_{l,k}^n = (\dot{x}_k^n(x_k^n - \chi_l) + \dot{y}_k^n(y_k^n - \psi_l))r_{l,k}^n$
    - $\tau_{l,k}^n = \text{round}(\frac{2\dot{r}_{l,k}^n/c}{\Delta\tau})$
    - $\nu_{l,k}^n = \text{round}(\frac{-2f_c\dot{r}_{l,k}^n/c}{\Delta\nu})$
    - $\mathbf{y}_{l,k}^n = |\frac{1}{M}\sum_{m=0}^{M} r(m)\bar{s}(m-\tau_{l,k}^n)e^{-j2\pi(m-\tau_{l,k}^n)\nu_{l,k}^n/M}|^2$
    - Obtain $\bar{\mathbf{y}}_{l,k}^n$ by thresholding $\mathbf{y}_{l,k}^n$
  - $w_k^n \propto w_{k-1}^n \prod_{l=1}^L \frac{p_1^n(\bar{\mathbf{y}}_{l,k}^n|\mathbf{x}_k^n)}{p_0^n(\bar{\mathbf{y}}_{l,k}^n|\mathbf{x}_k^n)}$

appears in the weight equation of the particle described later in this section. However, this likelihood is a multivariate exponential distribution [9] that grows in dimensionality as N increases. We assume that the measurements $\{\{\mathbf{y}_{l,k}^n\}_{n=1}^N\}_{l=1}^L$ are independent, which simplifies the likelihood for each particle to $\prod_{n=1,n\neq n'}^N \prod_{l=1}^L p_0^n(\mathbf{y}_{l,k}^n|\mathbf{x}_k^n)p_1^{n'}(\mathbf{y}_{l,k}^{n'}|\mathbf{x}_k^{n'})$, where $p_1^n(\mathbf{y}_{l,k}^n|\mathbf{x}_k^n)$ denotes the likelihood that a target exists at $\mathbf{x}_k^n$ and $p_0^n(\mathbf{y}_{l,k}^n|\mathbf{x}_k^n)$ denotes the likelihood that a target does not exist at $\mathbf{x}_k^n$. It can be shown that the covariance between two measurements $\mathbf{y}_{l,k}^{n'}, \mathbf{y}_{l,k}^n$ with $n' \neq n$, depends on the closeness of the two filters relative to the ambiguity function spread [10]. Therefore, the measurement independence assumption holds better for the Björck CAZAC and than for the LFM. Continuing with the likelihood, we have that:

$$p_1^n(\mathbf{y}_{l,k}^n|\mathbf{x}_k^n) = \tfrac{1}{2\sigma_1^2}e^{-\frac{\mathbf{y}_{l,k}^n}{2\sigma_1^2}} \quad \text{if target present}$$

$$p_0^n(\mathbf{y}_{l,k}^n|\mathbf{x}_k^n) = \tfrac{1}{2\sigma_0^2}e^{-\frac{\mathbf{y}_{l,k}^n}{2\sigma_0^2}} \quad \text{if target not present.}$$

Since the value of $\sigma_1^2 = \sigma_0^2(1 + \frac{2\sigma_A^2\xi^2}{\sigma_0}\mathcal{A}(\tau_{l,k}^n - \tau_{l,k}, \nu_{l,k} - \nu_{l,k}^n))$ is not known as the true target location $\tau_{l,k}, \nu_{l,k}$ is not known, thresholding of the matched filter output is required:

$$\bar{\mathbf{y}}_{l,k}^n(k) = \begin{cases} 1, & \text{if } \mathbf{y}_{l,k}^n \geq \mathcal{T} \\ 0, & \text{if } \mathbf{y}_{l,k}^n < \mathcal{T}. \end{cases}$$

The probability of detection is given by: $P_d = P_f^{1/(1+\text{SNR } \mathcal{A}(\tau_{l,k}^n - \tau_{l,k}, \nu_{l,k} - \nu_{l,k}^n))}$ and is calculated as an average over different values of $\tau_{l,k}^n - \tau_{l,k}, \nu_{l,k} - \nu_{l,k}^n$.

Following the proposal, each particle is weighted as:

$$w_k^n \propto w_{k-1}^n \frac{\prod_{n=1,n\neq n'}^N \prod_{l=1}^L p_0^n(\bar{\mathbf{y}}_{l,k}^n|\mathbf{x}_k^n)p_1^{n'}(\bar{\mathbf{y}}_{l,k}^{n'}|\mathbf{x}_k^{n'})p(\mathbf{x}_k|\mathbf{x}_{k-1}^n)}{q(\mathbf{x}_k|\mathbf{x}_{k-1}^n)}$$

which, with $q(\mathbf{x}_k|\mathbf{x}_{k-1}^n) = p(\mathbf{x}_k|\mathbf{x}_{k-1}^n)$, simplifies to

$$w_k^{n'} \propto w_{k-1}^{n'} \prod_{n=1}^N \prod_{l=1}^L p_0^n(\bar{\mathbf{y}}_{l,k}^n|\mathbf{x}_k^n)p_1^{n'}(\bar{\mathbf{y}}_{l,k}^{n'}|\mathbf{x}_k^{n'}).$$

Further modifying the weights by dividing the left hand side by the constant $\prod_{n=1}^N \prod_{l=1}^L p_0^n(\bar{\mathbf{y}}_{l,k}^n|\mathbf{x}_k^n)$, the weights for a particle is given by the simple expression

$$w_k^{n'} \propto w_{k-1}^{n'} \prod_{l=1}^L \frac{p_1^{n'}(\bar{\mathbf{y}}_{l,k}^{n'}|\mathbf{x}_k^{n'})}{p_0^{n'}(\bar{\mathbf{y}}_{l,k}^{n'}|\mathbf{x}_k^{n'})}.$$

Each particle then, represents a hypothesis on the delay and Doppler shift of the return signal due to the state of the target. A matched filter can, therefore, be placed at each of the pro-

posed delay and Doppler shifts proposed by the particles. This deviates from the traditional practice of evaluating matched filters exhaustively at regular intervals across the delay-Doppler space. In the particle filter case, the matched filters are not spread evenly in the delay-Doppler space, but are proposed at locations where a target is believed to exist at time step k. This also removes the need to design a tessellating shape to approximate probability of detection contours that introduces measurement errors. The algorithm is outlined in Table I.

B. Likelihood PF

In the Björck CAZAC case, the likelihood is very concentrated. Although this is good for measurement accuracy, the SIRPF will not work in this case as particles sampled from the broadly spread prior will not satisfy the likelihood easily. With the LPF we sample values from the likelihood as it is more concentrated than the prior in the Björck CAZAC case. To achieve this, we evaluate the likelihood values at discrete bins of the delay-Doppler space of size T and $\Delta\nu$. We create a histogram from these values and sample from it. To avoid, however, the exhaustive evaluation of the likelihood in the entire delay-Doppler space, we narrow our selection of bins to those that fall within the prior. Therefore, for each particle, we select a region within which a proposal from the prior would fall with probability of almost 1.

We begin by propagating the $x-y$ coordinate components of the state space without the addition of noise. This provides the mean of the Gaussian distribution from which we would sample from in the SIRPF case:

$$[\check{x}_k^n, \check{y}_k^n] = [x_{k-1}^n + \dot{x}_k^n \tau, y_{k-1}^n + \dot{x}_k^n \tau]. \tag{2}$$

From this, it follows that:

$$\check{r}_{l,k}^n = \sqrt{(\chi_l - \check{x}_k^n)^2 - (\psi_l - \check{y}_k^n)^2}. \tag{3}$$

If we assume for simplicity that $\sigma_x = \sigma_y$, then with probability of almost 1, the proposed particle will fall within $3\sigma_x$ from $\check{x}_k^n$ and similarly from $\check{y}_k^n$. Further assuming that the target is at angle $\pi/2$ with the sensor, the maximum and minimum possible sampled x and y coordinates would yield the maximum a minimum range as:

$$[r_{l,k,min}^n, r_{l,k,max}^n] = [\check{r}_{l,k}^n - 3\sqrt{2}\sigma_x, \check{r}_{l,k}^n + 3\sqrt{2}\sigma_x] \tag{4}$$

which implies minimum and maximum index values for the delay, and with a similar procedure for the Doppler:

$$[\tau_{l,k,min}^n, \tau_{l,k,max}^n] = [\text{round}(\frac{2r_{l,k,min}^n/c}{T}), \text{round}(\frac{2r_{l,k,max}^n/c}{T})] \tag{5}$$

$$[\dot{r}_{l,k,min}^n, \dot{r}_{l,k,max}^n] = [\dot{r}_{l,k}^n - 3\sqrt{2}\sigma_{\dot{x}}, \dot{r}_{l,k}^n + 3\sqrt{2}\sigma_{\dot{x}}] \tag{6}$$

$$[\nu_{l,k,min}^n, \nu_{l,k,max}^n] = [\text{round}(\frac{-2f_c\dot{r}_{l,k,min}^n/c}{\Delta\nu}), \text{round}(\frac{-2f_c\dot{r}_{l,k,max}^n/c}{\Delta\nu})] \tag{7}$$

We form sets of indices for delay and Doppler between the minimum and maximum allowable values as:

$$\tau_{l,k}^n = \{\tau_{l,k,min}^n + k_\tau\}_{k_\tau=0}^{\tau_{l,k,max}^n}, \nu_{l,k}^n = \{\nu_{l,k,max}^n + k_\nu\}_{k_\nu=0}^{\nu_{l,k,max}^n}.$$

Evaluating the matched filter output at each of these values we have:

$$\mathbf{y}_{k_\tau,k_\nu,l,k}^n = |\frac{1}{M}\sum_{m=0}^{M-1} d(m) s^*(m - \tau_{k_\tau,l,k}^n) e^{-j2\pi(m-\tau_{k_\tau,l,k}^n)\nu_{k_\nu,l,k}^n/M}|^2.$$

Furthermore, the likelihood using the independence assumption is given by:

TABLE II
LIKELIHOOD PARTICLE FILTER [5]

- For each particle $n = 1, \ldots, N$
  - $\check{\mathbf{x}}_k^n = \mathbf{F}\mathbf{x}_{k-1}^n$
  - For each sensor $l = 1, \ldots, L$
    - $\check{r}_{l,k}^n = \sqrt{(\chi_l - \check{x}_k^n)^2 + (\psi_l - \check{y}_k^n)^2}$
    - $\tau_{l,k}^n = \{\tau_{l,k,min}^n + k_\tau\}_{k_\tau=0}^{\tau_{l,k,max}^n}$
      $\nu_{l,k}^n = \{\nu_{l,k,max}^n + k_\nu\}_{k_\nu=0}^{\nu_{l,k,max}^n}$
      using (2), (3), (4), (5), (6), (7).
    - for $k_\tau = 0, \ldots, \tau_{l,k,max}^n$
    - for $k_\nu = 0, \ldots, \nu_{l,k,max}^n$
      - $\mathbf{y}_{k_\tau,k_\nu,l,k}^n(k) =$ $|\frac{1}{M}\sum_{m=0}^{M-1} d(m)$ $s^*(m - \tau_{k_\tau,l,k}^n) e^{-j2\pi(m-\tau_{k_\tau,l,k}^n)\nu_{k_\nu,l,k}^n/M}|^2$
      - $\beta_{\tau_{k_\tau},\nu_{k_\nu},l,k}^n = \frac{p_1^n(\mathbf{y}_{k_\tau,k_\nu,l,k}^n|\mathbf{x}_k^n)}{p_0^n(\mathbf{y}_{k_\tau,k_\nu,l,k}^n|\mathbf{x}_k^n)}$.
    - Sample $\tilde{k}_\tau, \tilde{k}_\nu \sim \{\{b_{k_\tau,k_\nu,l,k}^n\}_{k_\tau=0}^{\tau_{l,k,max}^n}\}_{k_\nu=0}^{\nu_{l,k,max}^n}$
    - $\tilde{r}_{l,k}^n = c\tau_{\tilde{k}_\tau}^n T/2,\ \tilde{\dot{r}}_{l,k}^n = c\nu_{\tilde{k}_\nu}^n \Delta\nu/(-2f_c)$
    - $\tilde{b}_{l,k}^n = b_{\tilde{k}_\tau,\tilde{k}_\nu,l,k}^n$
  - Calculate $\mathbf{x}_k^n$ based on $\tilde{r}_{l,k}^n$ and $\tilde{\dot{r}}_{l,k}^n$
  - $w_k^n \propto w_{k-1}^n p(\mathbf{x}_k^n|\mathbf{x}_{k-1}^n) \prod_{l=1}^L B_{l,k}^n$

$$p_1^n(\mathbf{y}_{k_\tau,k_\nu,l,k}^n|\mathbf{x}_k^n) = \frac{1}{2\sigma_1^2} e^{-\frac{\mathbf{y}_{k_\tau,k_\nu,l,k}^n}{2\sigma_1^2}} \quad \text{if target present}$$

$$p_0^n(\mathbf{y}_{k_\tau,k_\nu,l,k}^n|\mathbf{x}_k^n) = \frac{1}{2\sigma_0^2} e^{-\frac{\mathbf{y}_{k_\tau,k_\nu,l,k}^n}{2\sigma_0^2}} \quad \text{if target not present.}$$

Since the assumption is that a target is within the resolution cell with index k_τ, k_ν, $\tau_{l,k}^n - \tau_{l,k} = 0$ and $\nu_{l,k} - \nu_{l,k}^n = 0$. Therefore, in the expression of $\sigma_1^2 = \sigma_0^2(1 + \frac{2\sigma_A^2\xi^2}{\sigma_0}\mathcal{A}(\tau_{l,k}^n - \tau_{l,k}, \nu_{l,k} - \nu_{l,k}^n))$, we substitute $\mathcal{A}(\tau_{l,k}^n - \tau_{l,k}, \nu_{l,k} - \nu_{l,k}^n) = \mathcal{A}(0,0) = 1$. Unlike the case of the LFM, in the case of the Björck CAZAC, σ_1^2 is known. This allows us to use unthresholded measurements in the case of the Björck CAZAC for greater measurement accuracy.

After calculating the necessary likelihood values, we sample from it using the following process. Using the same assumptions for measurement independence as in the case of the SIRPF, we calculate the likelihood ratio as

$$\beta_{k_\tau,k_\nu,l,k}^n = \frac{p_1^n(\mathbf{y}_{k_\tau,k_\nu,l,k}^n|\mathbf{x}_k^n)}{p_0^n(\mathbf{y}_{k_\tau,k_\nu,l,k}^n|\mathbf{x}_k^n)}. \tag{8}$$

We normalize $\{\{\beta_{k_\tau,k_\nu,l,k}^n\}_{k_\tau=0}^{\tau_{l,k,max}^n}\}_{k_\nu=0}^{\nu_{l,k,max}^n}$. The normalization factor is

$$B_{l,k}^n = \sum_{k_\tau=0}^{\tau_{l,k,max}^n} \sum_{k_\nu=0}^{\nu_{l,k,max}^n} \beta_{k_\tau,k_\nu,l,k}^n \tag{9}$$

And the normalized distribution is:

$$b_{k_\tau,k_\nu,l,k}^n = \frac{\beta_{k_\tau,k_\nu,l,k}^n}{B_{l,k}^n}. \tag{10}$$

For each particle n we sample one set of indices $\tilde{k}_\tau, \tilde{k}_\nu \sim \{\{b_{k_\tau,k_\nu,l,k}^n\}_{k_\tau=0}^{\tau_{l,k,max}^n}\}_{k_\nu=0}^{\nu_{l,k,max}^n}$. The resulting sampled range and range rate and the bias are respectively: $\tilde{r}_{l,k}^n = c\tau_{\tilde{k}_\tau}^n T/2$, $\tilde{\dot{r}}_{l,k}^n = c\nu_{\tilde{k}_\nu}^n \Delta\nu/(-2f_c)$, $\tilde{b}_{l,k}^n = b_{\tilde{k}_\tau,\tilde{k}_\nu,l,k}^n$.

Although, the use of a CAZAC offers accuracy in the range and range rate, this does not imply accuracy in the location and velocity in the $x-y$ plane. However, with the use of two sensors and the intersections in the $x-y$ plane resulting from two range and range rate measurements, a high resolution in

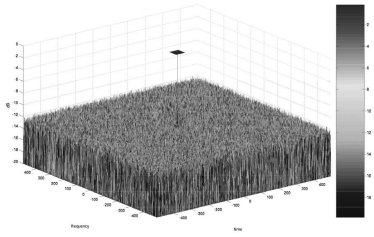

Fig. 1. Plot of the periodic ambiguity function of a Björck CAZAC sequence with $p = 101$ (the peak has been marked with a red square for legibility).

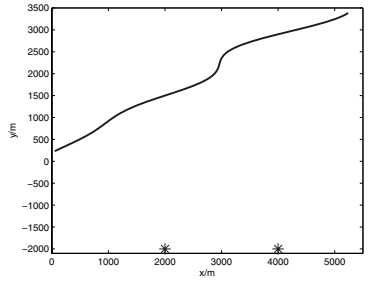

Fig. 2. Trajectory of a single target. The two sensors are indicated by a '*'.

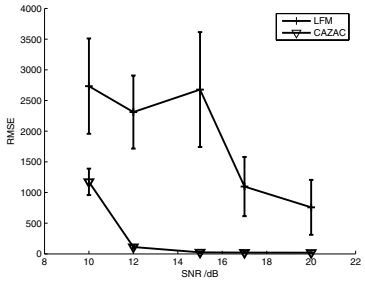

Fig. 3. RMSE versus SNR tracking performance in a single target tracking scenario.

the $x - y$ plane results.

Continuing with the method description, the values of $\tilde{r}^n_{l,k}$ and $\tilde{\dot{r}}^n_{l,k}$ yield proposed state values for location and velocity in the $x - y$ coordinates $\mathbf{x}^n_k$. Thus the weight equation of a particle, using likelihood ratios becomes

$$w^n_k \propto w^n_{k-1} \frac{\prod_{l=1}^{L} p^n_1(\mathbf{y}^n_{k_\tau,k_\nu,l,k}|\mathbf{x}^n_k) p(\mathbf{x}^n_k|\mathbf{x}^n_{k-1})}{\prod_{l=1}^{L} p^n_0(\mathbf{y}^n_{k_\tau,k_\nu,l,k}|\mathbf{x}^n_k) \prod_{l=1}^{L} \tilde{b}^n_{l,k}}.$$

Using equations (8)-(10), the weight equation simplifies to:

$$w^n_k \propto w^n_{k-1} p(\mathbf{x}^n_k|\mathbf{x}^n_{k-1}) \prod_{l=1}^{L} B^n_{l,k}.$$

The algorithm is outlined in Table II.

V. Simulation Results

A single target moves in a two-dimensional plane in the Cartesian coordinates. The motion is completed in 199 time steps. Two sensors located at $\chi_1 = 2000$ m, $\psi_1 = -2000$ m and $\chi_2 = 4000$ m, $\psi_2 = -2000$ m collect range and range rate measurements. The trajectory of the target and the location of the sensors are shown in Figure 2. The target is assumed to move according to a nearly constant velocity model with covariance matrix Q =diag(60 7 60 7). The SNR varies as $10, 12, 15, 17, 20$ dB. The P_f is set to 10^{-3}, which applies only in the case of the LFM waveform. Both waveforms have $M = 4999$ samples, are sampled at 10 MHz and frequency modulated by $f_c = 40$ GHz. The speed of propagation of the waveforms is $c = 2.997925 \times 10^8$ m/s. For the LFM waveform we set $f_a = 0.4$ and $f_b = 0.01$.

For the simulations, we used $N = 800$ particles and the results were averaged over 100 Monte Carlo runs. In Figure 3 the RMSE tracking performance is shown for different values of SNR and for both waveforms. We observe that the LPF with a Björck CAZAC clearly outperforms the SIRPF with an LFM waveform. It also produces more reliable estimates as shown by the much shorter confidence intervals.

VI. Conclusions

In this paper, we have applied two particle filtering methods (SIRPF and LPF) to the problem of tracking a single target using radar and explained the benefits of particle filtering over traditional approaches in radar tracking. We have investigated the validity of the assumptions that make the two methods computationally efficient when using an LFM waveform or a Björck CAZAC sequence, and examined the factors which affect the measurement accuracy in terms of resolution in the delay-Doppler space and the use of measurement thresholding. Moreover, we have performed simulations to investigate the tracking performance resulting from the use of these signals.

We have shown how the particle filtering method outperforms matched filtering operations by concentrating in areas where a target is believed to exist and avoiding the exhaustive evaluation on a grid in the delay-Doppler space. As a consequence, the necessity to approximate probability of detection contours by tessellating shapes such as a parallelograms is avoided. This results to higher measurement accuracy.

We also demonstrate that Björck CAZACs provide higher measurement accuracy than LFM waveforms, due to their localized ambiguity function which also justifies the use of unthresholded measurements. Moreover, assumptions of measurement independence are approximately true for Björck CAZACs, making them a computationally efficient choice for target tracking using a particle filter. We show through simulation results that Björck CAZACs attain a significantly better performance level than the LFM.

References

[1] N. Levanon and E. Mozeson, "Radar Signals." Wiley, 2004.

[2] G. Björck, "Functions of modulus one on $\mathbb{Z}_n$ whose Fourier transforms have constant modulus, and cyclic n-roots," *Proc. of 1989 NATO Advanced Study Institute on Recent Advances in Fourier Analysis and Its Applications*, J.S. Byrnes and J. L. Byrnes, ed. pp 131-140, 1990.

[3] C. Rago, P. Willett, Y. Bar-Shalom, "Detection-tracking performance with combined waveforms," *IEEE Trans. on Aerospace and Electronic Systems,* vol. 34, no. 2, pp. 612 - 624, April 1998.

[4] Ruixin Niu, P. Willett, Y. Bar-Shalom, "Tracking considerations in selection of radar waveform for range and range-rate measurements," *IEEE Trans. on Aerospace and Electronic Systems*, vol. 38, no. 2, pp. 467 - 487, April 2002.

[5] M. S. Arulampalam, S. Maskell, N. Gordon, and T. Clapp "A Tutorial on Particle Filters for Online Nonlinear/Non-Gaussian Bayesian Tracking", *IEEE Transactions on Signal Processing*, vol. 50, no. 2, pp. 174-188, Feb. 2002.

[6] M. I. Skolnik, "Introduction to radar systems," McGraw-Hill, 1980.

[7] D. Chu, "Polyphase codes with good periodic correlation properties," *IEEE Transactions on Information Theory (Corresp.)*, vol. 18, no. 4, pp. 531 - 532, Jul. 1972.

[8] J.J. Benedetto, J. Donatelli, I. Konstantinidis and C. Shaw, "A Doppler statistic for zero autocorrelation waveforms," *40th Annual Conference on Information Sciences and Systems*, pp. 1403 - 1407, March 2006.

[9] R.K. Mallik, "On multivariate Rayleigh and exponential distributions," *IEEE Transactions on Information Theory*, vol. 49, no. 6, pp 1499 - 1515, June 2003.

[10] Ioannis Kyriakides, Darryl Morrell and Antonia Papandreou-Suppappola, "On the Validity of the Measurement Independence Assumption When Using CAZAC and LFM Waveforms in Radar Tracking With a Particle Filter", Technical Report EEE-4-9-2007-1, Dept. of Electrical Engineering, Arizona State University, April 2007. `http://www.public.asu.edu/~ikyriaki`.